

# Pulsed laser deposition of Ni-Mn-Ga thin films on silicon

A. Hakola<sup>1</sup>, O. Heczko<sup>1</sup>, A. Jaakkola<sup>1</sup>, T. Kajava<sup>1</sup>, and K. Ullakko<sup>2</sup>

<sup>1</sup> Department of Engineering Physics and Mathematics, Helsinki University of Technology, P.O.Box 2200, FIN-02015 HUT, Finland, fax: +358-9-451 3195, e-mail: Antti.Hakola@hut.fi

<sup>2</sup> AdaptaMat Ltd., Yrityspiha 5, FIN-00390, Helsinki, Finland

Received: date / Revised version: date

**Abstract** Thin films of magnetic shape-memory (MSM) material Ni-Mn-Ga have been deposited on Si(100) substrates using pulsed laser deposition. The 200–300-nm-thick films were prepared at substrate temperatures ranging from 450 °C to 650 °C and at different background Ar pressures. Large saturation magnetizations, up to 60% of the bulk value were measured for the films. Only the films deposited in vacuum or at Ar pressures below  $10^{-3}$  mbar and at temperatures between 500 °C and 600 °C were ferromagnetic. The films are mainly crystallized in the austenitic phase and they have a smooth surface with a low droplet density ( $0.01 \mu\text{m}^{-2}$ ). The magnetization and surface quality are sufficient that the films could be utilized in the realization of thin-film MSM devices.

---

PACS: 75.70.Ak

## 1 Introduction

Stoichiometric Ni<sub>2</sub>MnGa and other Ni-Mn-Ga alloys are intensively studied ferromagnetic shape-memory materials which exhibit large magnetic-field-induced strains [1]. The phenomenon is based on the motion of martensitic twin variants in an applied magnetic field, which gives rise to the macroscopic shape change [1–3]. The largest magnetostrain, almost 10%, has been induced in off-stoichiometric Ni<sub>48.8</sub>Mn<sub>29.7</sub>Ga<sub>21.5</sub> [4].

This magnetic shape-memory (MSM) effect provides a new way to generate motion and force without moving parts and, consequently, makes it possible to design and realize novel actuators and sensors [5, 6]. The main advantages of MSM materials are that they show much larger strains at room temperature than, e.g., traditional magnetostrictive materials and that they have a fast, less than 1 ms, response to the driving force. Ni-Mn-Ga is the most promising MSM material since it has a low hysteresis and the martensitic transition temperature can be easily adjusted by only varying the composition [7, 8].

So far most of the Ni-Mn-Ga research has dealt with bulk material. However, thin films would make it possible to realize microscopic components in a small volume by utilizing lithographic techniques [9]. In addition, MSM materials in thin-film form provide a possibility to integrate mechanical elements with semiconductors for novel micromechanical or microelectromechanical devices [10]. Ni-Mn-Ga films have been prepared by molecular beam epitaxy (MBE) [10–13], magnetron sputtering [8, 14], and pulsed laser deposition (PLD) [15–17] but to our knowledge no MSM effect has been observed.

We have deposited thin Ni-Mn-Ga films by PLD on silicon to find optimal values for the different deposition parameters, such as the substrate temperature, the laser fluence, and the background gas pressure. The aim was to produce ferromagnetic films with a smooth surface and the desired crystal structure. Silicon was chosen as the substrate material since it has a relatively good lattice match with bulk Ni-Mn-Ga and since standard lithographic techniques can be used to pattern small structures in the film.

## 2 Experimental

The films were deposited in an ultra-high vacuum PLD chamber originally designed to produce epitaxial multi-layer structures on up to 5-cm-diameter substrates [18]. A KrF excimer laser (Lambda Physik COMPex 205) produces 600-mJ laser pulses at 248 nm. The laser pulses were spatially shaped by a rectangular  $6 \times 12\text{-mm}^2$  aperture and imaged on the target surface to produce a flat-top distribution with an area of approximately  $3 \text{ mm}^2$ . In these experiments, the fluence was  $2.5\text{--}3 \text{ J/cm}^2$ . Typically, 200–300-nm-thick films were obtained with 40000 pulses.

The targets were 30-mm-diameter and 3-mm-thick slices cut from a single-crystalline Ni-Mn-Ga ingot. The ingots were manufactured by AdaptaMat Ltd. in a crystal growth furnace, and the target slices were cut from

a heat-treated ingot by spark-cutting equipment. The targets were mounted in a rotating holder to ensure uniform wear of the target. The small ( $0.5\text{--}1\text{-cm}^2$ ) Si(100) substrates were attached to a deposition plate made of Haynes alloy with silver paste to ensure a proper thermal contact during the film growth. The experiments were carried out both in vacuum (base pressure  $< 5 \times 10^{-6}$  mbar) and at different argon background pressures ( $3 \times 10^{-4}\text{--}5 \times 10^{-3}$  mbar). The substrate temperatures ranged from  $450\text{ }^\circ\text{C}$  to  $650\text{ }^\circ\text{C}$ . The target-substrate distance was 50 mm. We also varied this distance within a small range (45–60 mm) but did not observe any noticeable changes in the magnetic properties of the films.

Some of the films were annealed at high temperatures after their magnetic characterization. The samples were sealed in quartz vacuum ampoules and put in a furnace kept at a constant temperature of  $800\text{ }^\circ\text{C}$ . In some of the ampoules, we also put a piece of manganese or Ni-Mn-Ga to compensate for the possible evaporation of Mn during the heat treatment. The annealing times ranged from 15 min to 30 min.

The surface morphology of the films was studied with a LEO-1450 scanning electron microscope (SEM), and the chemical composition was determined by using energy dispersive spectroscopy (EDS). The crystal structure was analyzed by a Phillips X'pert X-ray diffractometer with  $\text{CoK}_\alpha$  radiation. The magnetization curves were measured with a vibrating sample magnetometer (VSM) in magnetic fields up to 1.43 T.

### 3 Results and discussion

Figure 1 shows a typical SEM image of a Ni-Mn-Ga film. The surface is relatively smooth but a few micron-diameter droplets can be seen on it. From these first deposited films, we obtained a rough order-of-magnitude estimate for the droplet density,  $0.01\text{ }\mu\text{m}^{-2}$ . An EDS analysis of one of the films at two different locations gave Ni/Mn/Ga compositions 46/31/23 and 46/30/24, which are close to the target composition 48.9/30.8/20.3. Also the compositions of other analyzed samples were similar to that of the target.

X-ray diffractograms of two Ni-Mn-Ga films with different thickness (100 nm and 300 nm) are shown in Figure 2. The distinctive peaks in the polycrystalline pattern allow one unequivocally to identify the  $L2_1$  cubic phase (corresponding to peaks labelled with ‘‘austenite’’) with a lattice constant of 0.580 nm. This value is close to that of bulk austenite (0.584 nm) [19]. Moreover, weak but discernible superstructure lines (111) and (200) at  $2\theta = 31.2^\circ$  and  $2\theta = 76.5^\circ$ , respectively, indicate that some degree of structural order has been established in the austenitic phase. The additional peaks in the diffractogram suggest the presence of another cubic,  $L2_1$  phase with a lattice constant of 0.539 nm – close to that of silicon (0.543 nm). This phase exists as an intermediate

layer that is probably created due to a lattice mismatch between the austenite and silicon.

Figure 3 shows the magnetization curves of a Ni-Mn-Ga film deposited at  $550^\circ\text{C}$ . The curve is measured by applying the magnetic field parallel ( $H_{\parallel}$ ) and perpendicular ( $H_{\perp}$ ) to the film plane. The in-plane curve is square-like and narrow. This suggests that the film consists of a single magnetically soft phase with small magnetic anisotropy. The curve measured in the perpendicular direction is tilted mainly due to the demagnetizing field. The effect of the demagnetizing field ( $N \cdot M$ , where  $N$  is the demagnetizing factor and  $M$  is the magnetization) on the magnetic field inside the sample is large for thin films since  $N \approx 1$  in the perpendicular direction whereas in the parallel direction  $N \approx 0$ . With a typical film thickness of 300 nm, the film area of  $0.5\text{ cm}^2$ , and the bulk density of Ni-Mn-Ga ( $8\text{ g/cm}^3$ ), we obtain a saturation magnetization of 34 emu/g, which is about 60% of the bulk value (60 emu/g). This value is a factor of 6 larger than what have been obtained earlier by PLD [15, 16] and of the same order of magnitude as for the films deposited by MBE [10–12].

In Figure 4, the in-plane magnetization curves of Ni-Mn-Ga films deposited at different temperatures and at different background gas pressures are compared. One can notice that increasing the substrate temperature from  $500\text{ }^\circ\text{C}$  to  $550\text{ }^\circ\text{C}$  has a significant effect on the saturation magnetization: an increase from less than 6 emu/g to 34 emu/g. This behavior is in good agreement with the results of Castaño et al. [16] and it suggests that at higher deposition temperatures the film tends to crystallize in the desired (austenitic) phase. However, when further increasing the deposition temperature, the ferromagnetic behavior degrades; The films prepared at temperatures higher than  $650\text{ }^\circ\text{C}$  were non-ferromagnetic. Annealing the samples at  $800\text{ }^\circ\text{C}$  had similar effects: even the shortest annealing times resulted in the disappearance of ferromagnetism. As the ferromagnetism in Heusler Ni-Mn-Ga alloys is due to the presence of Mn, this either suggests that Ni-Mn-Ga reacts with silicon producing a non-Heusler compound or that Mn evaporates from the film. An interesting observation was that only the films deposited with fluences close to  $3\text{ J/cm}^2$  were ferromagnetic implying that the fluence has to be high enough to produce a Heusler structure with correct Ni/Mn/Ga composition. Figure 4 also shows that the highest magnetization was obtained when the film was prepared in vacuum. An increase in the Ar background pressure decreased magnetization and at pressures above  $10^{-3}$  mbar the deposited films turned out to be non-ferromagnetic. A possible explanation is that at high pressures the energy distribution of the different elements and ionized species in the plasma plume changes due to collisions and reactive secondary scattering [20]. No changes in the magnetization curves were observed while cooling the samples down to 10 K. This indicates

that no martensitic transformation occurs, which is possibly due to the elastic constraint set by the substrate.

#### 4 Conclusions

We have studied the effect of different parameters on the crystalline quality and magnetic properties of Ni-Mn-Ga thin films deposited on silicon. We have found an optimal deposition-temperature window to produce films with large magnetizations, up to 60% of the value of bulk austenite. The films have a proper austenitic structure and a sufficiently smooth surface, which are important for the future fabrication of MSM devices.

#### References

1. K. Ullakko, J. K. Huang, C. Kantner, R. C. O'Handley, V. V. Kokorin: *Appl. Phys. Lett.* **69**, 1966 (1996).
2. R. C. O'Handley: *J. Appl. Phys.* **83**, 3263 (1998).
3. O. Heczko, A. Sozinov, K. Ullakko: *IEEE Trans. Magn.* **36**, 3266 (2000).
4. A. Sozinov, A. A. Likhachev, N. Lanska, K. Ullakko: *Appl. Phys. Lett.* **80**, 1746 (2002).
5. J. Tellinen, I. Suorsa, A. Jääskeläinen, I. Aaltio, K. Ullakko: in *Proc. ACTUATOR 2002, Int. Conf., Bremen, Germany, 2002*, p. 566.
6. P. Krulevitch, A. P. Lee, P. B. Ramsey, J. C. Trevino, J. Hamilton, M. A. Northrup: *J. Microelectromech. Syst.* **5**, 270 (1996).
7. C. Jiang, G. Feng, S. Gong, H. Xu: *Mat. Sci. Eng.* **A342**, 231 (2003).
8. I. Takeuchi, O. O. Famodu, J. C. Read, M. A. Aronova, K.-S. Chang, C. Craciunescu, S. E. Lofland, M. Wuttig, F. C. Wellstood, L. Knauss, A. Orozco: *Nature Materials* **2**, 180 (2003).
9. K. Bhattacharya, A. DeSimone, K. F. Hane, R. D. James, C. J. Palmstrøm: *Mat. Sci. Eng. A* **273-275**, 685 (1999).
10. J. W. Dong, L. C. Chen, C. J. Palmstrøm, R. D. James, S. McKernan: *Appl. Phys. Lett.* **75**, 1443 (1999).
11. J. W. Dong, L. C. Chen, J. Q. Xie, T. A. R. Müller, D. M. Carr, C. J. Palmstrøm, S. McKernan, Q. Pan, R. D. James: *J. Appl. Phys.* **88**, 7357 (2000).
12. J. W. Dong, J. Lu, J. Q. Xie, L. C. Chen, R. D. James, S. McKernan, C. J. Palmstrøm: *Physica E* **10**, 428 (2001).
13. Q. Pan, J. W. Dong, C. J. Palmstrøm, J. Cui, R. D. James: *J. Appl. Phys.* **91**, 7812 (2002).
14. S. I. Patil, D. Tan, S. E. Lofland, S. M. Bhagat, I. Takeuchi, O. Famodu, J. C. Read, K.-S. Chang, C. Craciunescu, M. Wuttig: *Appl. Phys. Lett.* **81**, 1279 (2002).
15. P. G. Tello, F. J. Castaño, R. C. O'Handley, S. M. Allen, M. Esteve, F. Castaño, A. Labarta, X. Batlle: *J. Appl. Phys.* **91**, 8234 (2002).
16. F. J. Castaño, B. Nelson-Cheeseman, R. C. O'Handley, C. A. Ross, C. Redondo, F. Castaño: *J. Appl. Phys.* **93**, 8492 (2003).
17. V. Podgurski, S. Galambos: in *Proc. DAAAM, Int. Conf., Tallinn, Estonia, 2000*, p. 229.
18. M. Tuohiniemi, T. Kajava, T. Katila, M. M. Salomaa, R. Salomaa, E. Supponen: *Appl. Phys. A* **69**, S451 (1999).
19. O. Heczko, N. Lanska, O. Söderberg, K. Ullakko: *J. Magn. and Magn. Mat.* **242-245**, 1446 (2002).
20. D. B. Chrisey, G. K. Hubler (editors): *Pulsed Laser Deposition of Thin Films* (Wiley, New York, 1994) 455-471.

**Fig. 1** Scanning electron microscope image of a Ni-Mn-Ga film in a 20- $\mu\text{m}$  scale.

**Fig. 2** X-ray diffractograms of two Ni-Mn-Ga films with thicknesses 100 nm and 300 nm.

**Fig. 3** Magnetization curves of a Ni-Mn-Ga thin film deposited at 550°C. The curve is measured at room temperature in the film plane (open circles) and perpendicular to it (solid circles).

**Fig. 4** Room-temperature in-plane magnetization curves of Ni-Mn-Ga films deposited at 500°C (open triangles), at 550°C (solid squares), at 600°C (solid circles), and at 550°C using a  $3 \times 10^{-4}$ -mbar Ar pressure (open circles).

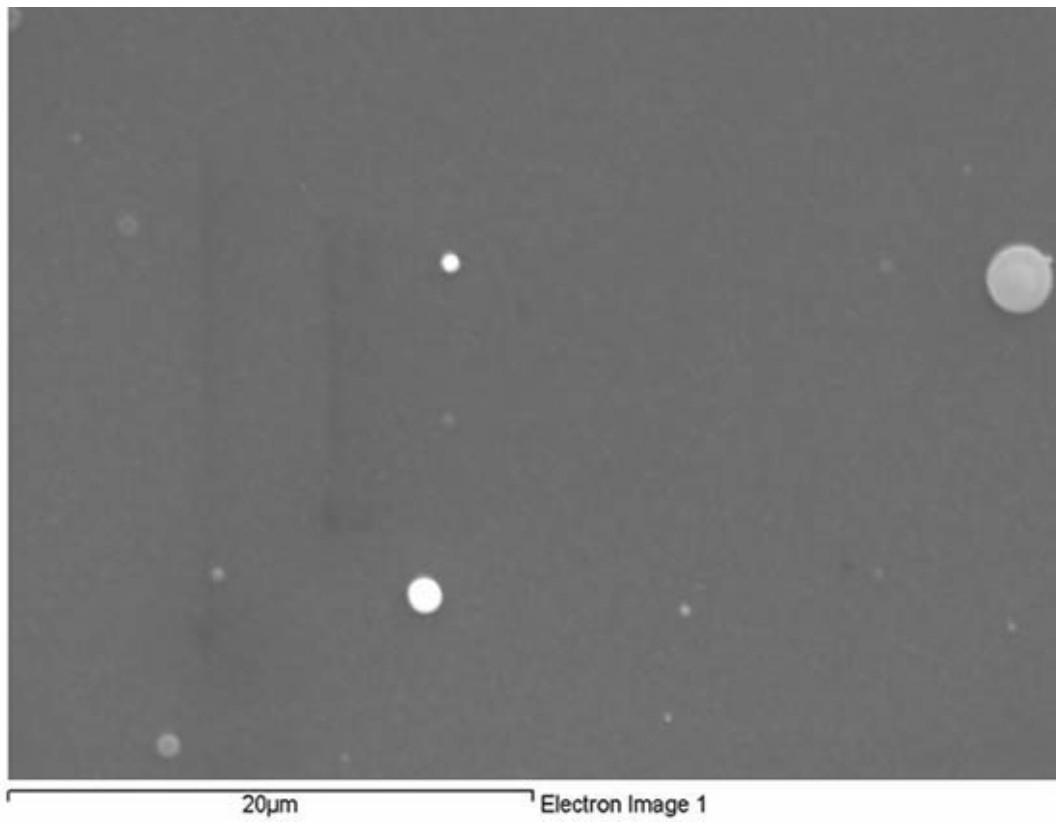


Figure 1. A. Hakola et al., Appl. Phys. A

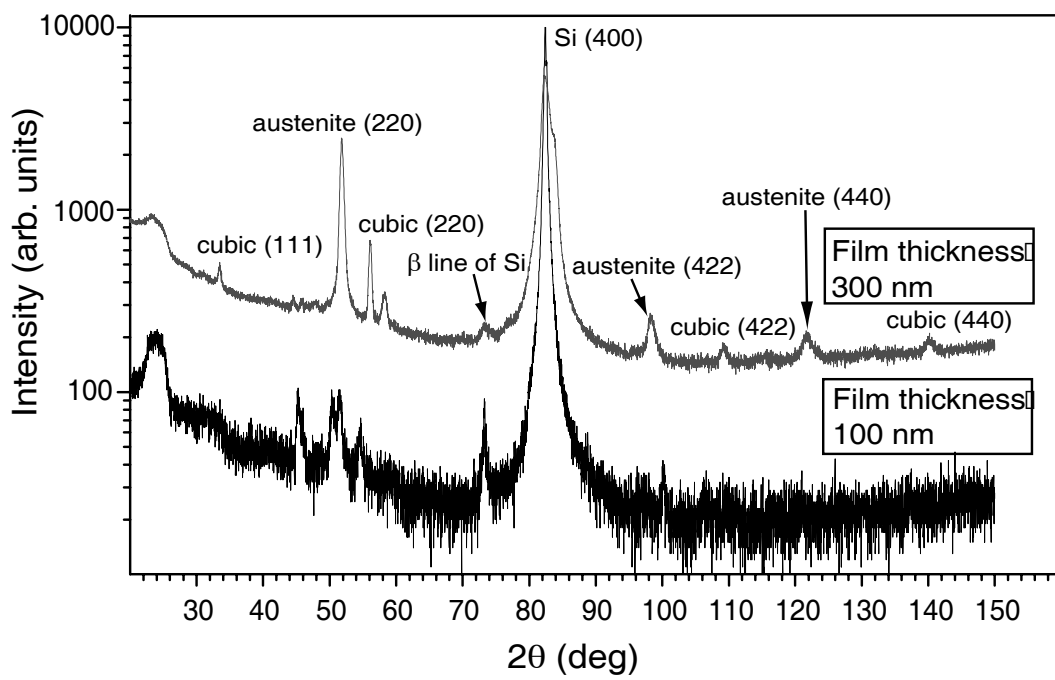


Figure 2. A. Hakola et al., Appl. Phys. A

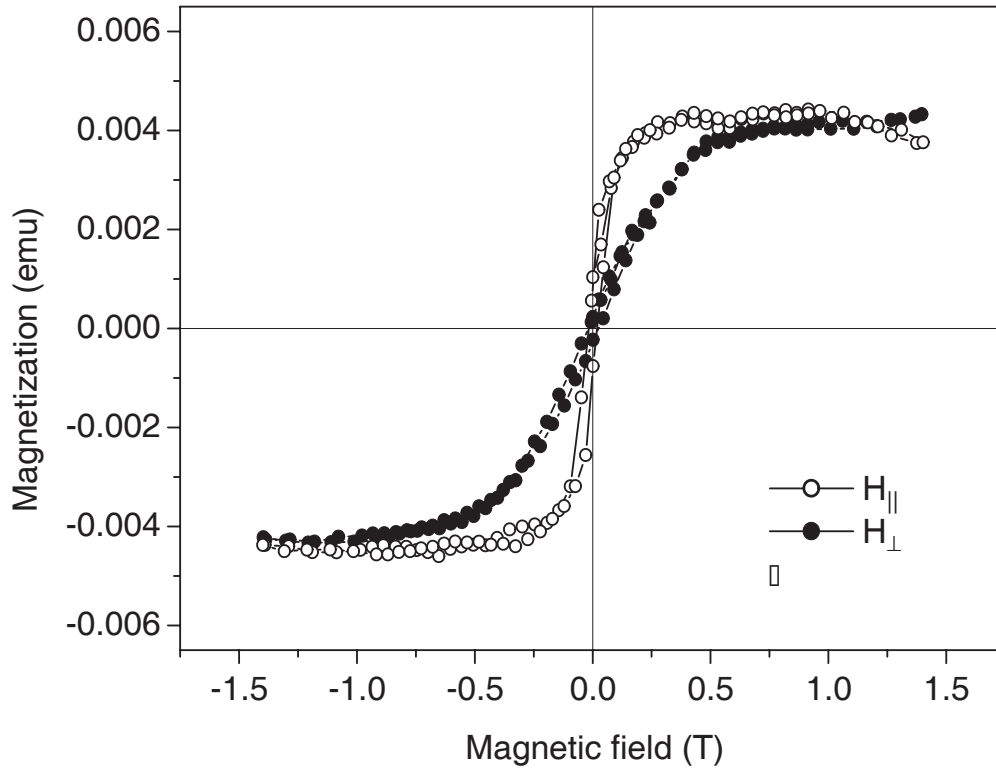


Figure 3. A. Hakola et al., Appl. Phys. A

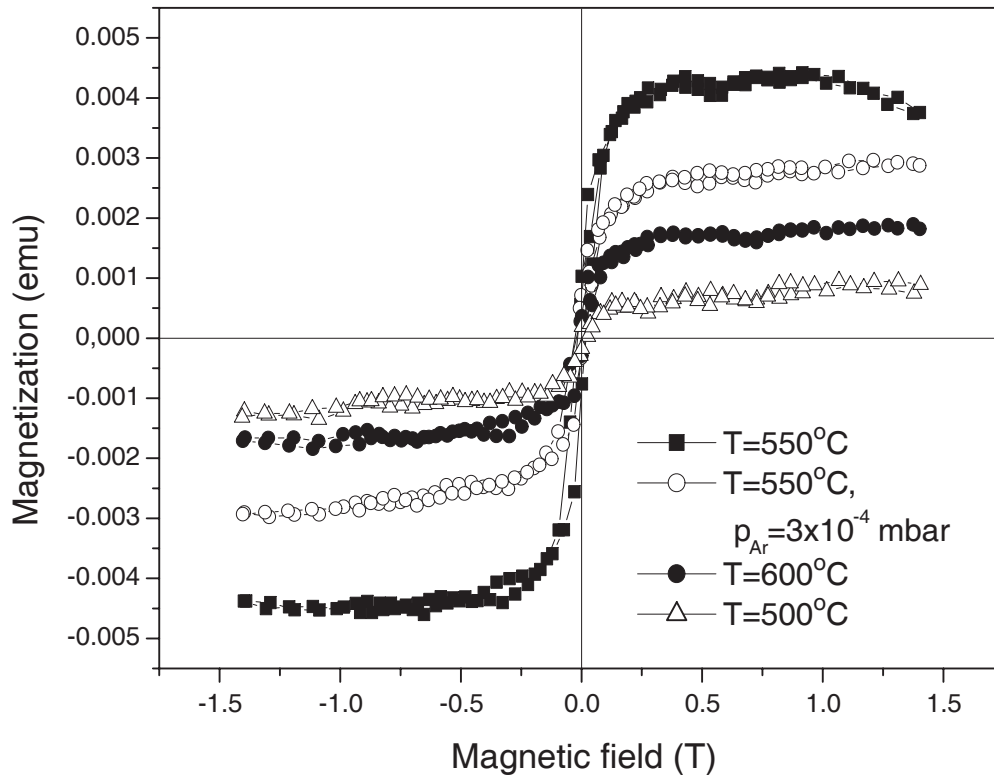


Figure 4. A. Hakola et al., Appl. Phys. A